Self-sealing experiments with water and gas injection on Callovo-Oxfordian claystone under X-ray tomography

Mensan Dèlwindé Gildas Cedric Agboli
Université de Lorraine, CNRS, Laboratoire GeoRessources, Nancy, France

Dragan Grgic
Université de Lorraine, CNRS, Laboratoire GeoRessources, Nancy, France

Albert Giraud
Université de Lorraine, CNRS, Laboratoire GeoRessources, Nancy, France

ABSTRACT: Self-sealing tests with water injection were performed on artificially fractured core samples of the Callovo-Oxfordian claystone using an X-ray transparent triaxial cell. 3D X-ray scans and permeability measurements were performed continuously to assess the evolution of fracture volume and permeability. The impact of sample orientation (parallel and perpendicular to the bedding plane), calcite content and gas injection was analyzed. It resulted that the higher the calcite content, the less effective the self-sealing process. No significant influence of the sample orientation on the self-sealing process was identified. Self-sealing is generally fast at the beginning of the test and then stabilizes after one month. The initial permeability of the healthy claystone is partially restored, which is a promising result concerning the restoration of the initial sealing properties of the host rock. Injection of an inert gas has a delay effect on the self-sealing process due to the crack desaturation.

Keywords: X-ray tomography, self-sealing, permeability, claystone, calcite content.

1 INTRODUCTION

Excavation of underground galleries can result in the formation of an Excavation Damaged Zone (EDZ), which is a network of cracks in the surrounding rock. These flaws desaturate the host rock and can cause a deterioration of its mechanical and hydraulic (i.e., low permeability) properties. In the case of Underground Research Laboratory (URL) of the National Agency of Radioactive waste Management (ANDRA) located in Meuse/Haute-Marne (Bure, France) and excavated in the Callovo-Oxfordian (COx) claystone, the structures will be resaturated and during this stage the cracks in the EDZ can self-seal, resulting in a decrease in water permeability and a partial restoration of the rock's mechanical properties. In the context of radioactive waste disposal, knowing this long-term self-sealing phenomenon is of great importance.

Many scholars have investigated the occurrence of self-sealing fractures in claystone caused by water percolation. Self-sealing is induced by a rearrangement of minerals and pores inside the fracture region, according to Auvray et al. (2015). Hence, these structural changes are expected to ameliorate mechanical and transfer properties of the fractured zone. Bastiaens et al. (2007) defined

self-sealing as the lowering of permeability in the EDZ by any hydro-mechanical-bio-chemical mechanism. Furthermore, Bastiaens et al. (2007) and Van Geet et al. (2008) investigated in-situ studies on Opalinus clay and Boom clay presenting their capabilities to self-seal rather than self-restore. De La Vaissière et al. (2015) have shown the partial restoration of the permeability of the COx claystone during in-situ resaturation experiments. Over a year, the hydraulic conductivity in the boreholes reduced by up to four orders of magnitude, nearing the value of healthy claystone, demonstrating the COx claystone's potential to self-seal.

While various studies have demonstrated claystone's capacity to self-seal, there is little information on how different parameters, such as the fluid nature, sample orientation and calcite content, impact the self-sealing process. Auvray et al. (2015) performed self-sealing tests on the COx argillite in a PEEK triaxial cell with only 2D X-ray scans. Giot et al. (2019) performed comparable studies with 3D X-ray scans but with basic voxel data analysis. In these studies, only clayey facies of COx claystone was tested. The purpose of our research is to investigate the impact of different parameters on the self-sealing process of artificially fractured core samples of COx claystone. Then, two types of self-sealing tests will be performed on the COx claystone. First, tests with water injection and different samples orientations (i.e., parallel and perpendicular to the bedding plane) and calcium carbonates (calcite) contents. Second, a test with injection of both water and gas to investigate the effect of gas injection on the self-sealing process. 3D X-ray scans will be performed on all tested samples before, during and after the experiments. The voxel data will be analyzed with a specific software for the visualization and analysis of computed tomography (CT) data in order to assess the evolution of the crack volume. Fracture permeability (to water and gas) will be measured continuously during all tests.

2 MATERIAL AND METHODS

2.1 COx claystone

Callovo-Oxfordian claystone is a very low-permeability rock whose mineral composition varies as a function of depth. The clay minerals content is approximately anti-correlated with the carbonates content. The three main mineral phases are clays, quartz, and calcite, with a high content of swelling clay minerals (smectites). The porosity of the COx claystone is about 18% and the water permeability ranges from 10^{-20} m^2 to 10^{-21} m^2. The synthetic water of ANDRA, whose chemical composition is close to in-situ porewater at the ANDRA URL, is used in our experiments to prevent any structural damage due to geochemical reactions.

ANDRA boreholes were used to core cylindrical samples of 20 mm diameter and 40 mm height for the self-sealing tests. Two sample orientations were considered, namely parallel and perpendicular to the bedding plane. These core samples were purposely fractured. First, samples were sawn in two along a plane containing the axis of the cylinder. Second, one of the faces was machined by milling with a high precision tool in order to obtain an artificial crack on a one-third of the diameter with an opening of 400 µm (Fig. 1). We chose an aperture of 400 µm for the initial crack according to previous works (Auvray et al. 2015 and Giot et al. 2019) and ANDRA's recommendations. Therefore, the initial crack has a theoretical initial volume equal to 106.5 mm^3.

2.2 Experimental device

We developed a mini-triaxial cell in which cylindrical specimens of diameter 20 mm and height 40 mm can be tested. The body of this cell is made of PEEK CF30 (PolyEtherEtherKetone, 30% carbon fibers) and is therefore transparent to X-rays, thus allowing 3D scans in a X-ray computed tomography scanner (GE Phoenix Nanotom S CT scanner, Fig. 1) with a voxel resolution of 24 µm. After 3D reconstruction of the sample volume, images were analyzed with the VGStudio MAX Software (Volume Graphics GmbH), which allows isolation and visualization of the fracture and the quantification of its volume.

At both end caps (outlets) of the triaxial cell, drainage holes allow to inject different fluids (water or gas) at different pressures in the sample during self-sealing tests. Upstream and downstream fluids pressures are controlled with high precision syringe pumps and exchanged fluid volumes are continuously recorded, thus allowing the measurement of fluid flow rate and then permeability.

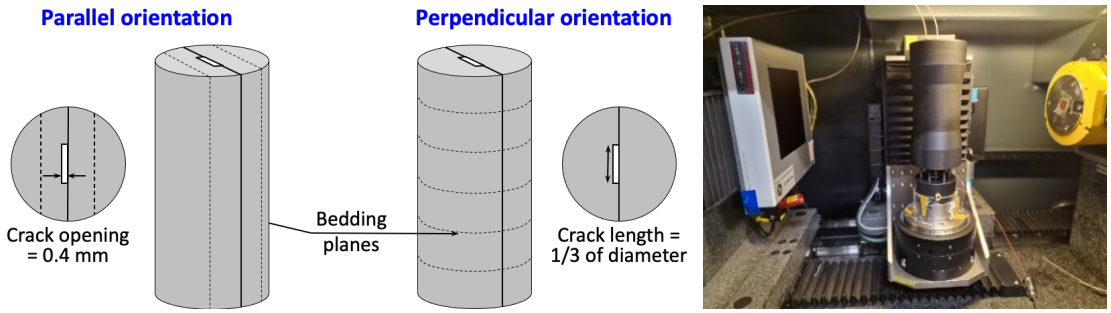

Figure 1. Left: Geometry of the artificially fractured cylindrical samples (Ø = 20 mm; h = 40 mm) for self-sealing tests. Right: PEEK triaxial compression cell for self-sealing tests in an X-ray nano-tomograph.

2.3 Experimental protocol

The artificially fractured sample is put in the PEEK triaxial cell (separated from the surrounding oil by a waterproof Viton© membrane) and a confining pressure of 4 MPa, corresponding to the pressure applied on the galleries wall by swelling clays (bentonite) of the plug, is applied. Then, a first 3D X-ray scan is performed to record the crack's initial shape. Next, synthetic water is injected from the bottom (upstream) of the sample at a constant rate of 0.05 ml/min in order to saturate the fracture. After saturation, a second 3D X-ray scan is performed. Then, water circulation is imposed in the fractured sample with a water pressure gradient of 0.2 MPa (upstream/bottom pressure = 1 MPa; downstream/top pressure = 0.8 MPa). As soon as steady state flow is achieved, water permeability can be measured. Concerning the self-sealing test with water and gas injection, the same procedure was followed, except that an inert gas (nitrogen) is injected into the sample (from the bottom) at different times, with a bottom/upstream pressure of 0.2 MPa or 0.5 MPa (depending on the level of sealing), while the top/downstream is left at atmospheric pressure. During these gas injection stages, gas removes first the water filling the crack and the tubing and, next, can flow continuously through the sample. Once a steady state gas flow is achieved, gas permeability can be measured. All self-sealing tests were carried out at 20°C and last at least one month.

The water permeability k_w of the cracked samples was calculated from the volumes measured at both upstream and downstream sides of the sample. It is based on a steady-flow approach taking into consideration Darcy's law. The gas permeability k_g is calculated at equilibrium using Darcy's equation for compressible gas flow. Both permeabilities are given by the equation (1) below:

$$k_w = \frac{Q\mu L}{S(P_u - P_d)} \qquad k_g = \frac{2\mu Q L P_u}{S(P_u^2 - P_d^2)} \tag{1}$$

Where k_w and k_g are the intrinsic permeabilities (m^2), Q the volumetric flow rate ($m^3.s^{-1}$), μ the liquid (water or gas) dynamic viscosity (Pa.s), S the injection surface of the sample (m^2), L the length of the sample (m), and P_u and P_d the upstream and downstream fluid (water or gas) pressures (Pa).

Because we are measuring the water flow rate in a fractured porous sample and since the Darcy law describes the flow across a porous medium, the permeability k_w corresponds here to the "apparent permeability" of a fractured sample. However, because the matrix permeability of this claystone is very low (less than 10^{-20} m^2), the observed permeability corresponds probably to the crack permeability. Moreover, the measured gas permeability is actually the apparent gas permeability. However, because the gas flow occurs mostly in a large crack, the Klinkenberg or slippage effect (Klinkenberg 1941) is likely negligible here. Then, we can consider that the measured permeability is the intrinsic permeability and represents the fracture permeability (the gas flow occurs mainly in the crack).

3 RESULTS AND DISCUSSION

3.1 Experimental results

Five self-sealing tests with water injection were performed on COx claystone samples with different orientations and calcite contents: EST60766-3 (parallel, %CaCO3 = 21), EST63744-7 (parallel, %CaCO3 = 32), EST63744-11 (perpendicular, %CaCO3 = 32), EST60007-71 (perpendicular, %CaCO3 = 53) and EST59996-71 (perpendicular, %CaCO3 = 68). The evolution of the water permeability is presented in Figure 2 (left). Only the downstream curves were represented (the upstream curves are almost the same). Concerning very carbonated samples (EST60007-71 and EST59996-71), self-sealing was very moderate and the fracture remained globally open. Therefore, no water permeability measurements could be performed since the flow rate was too fast.

X-ray 3D tomography images of parallel sample EST60766-3 showing the evolution of the crack volume with time during self-sealing test are represented in Figure 3 (left). Figure 3 (right) represents the volume variation percentage of the initial crack (normalized with the volume after hydrostatic loading) obtained from X-ray tomography 3D images during all self-sealing tests with water. The hydrostatic loading at a confining pressure of 4 MPa and the sample saturation induced a partial closure of the initial crack. The mechanical closure due to the confining pressure is much more efficient for the parallel sample, probably because of the clay minerals orientation.

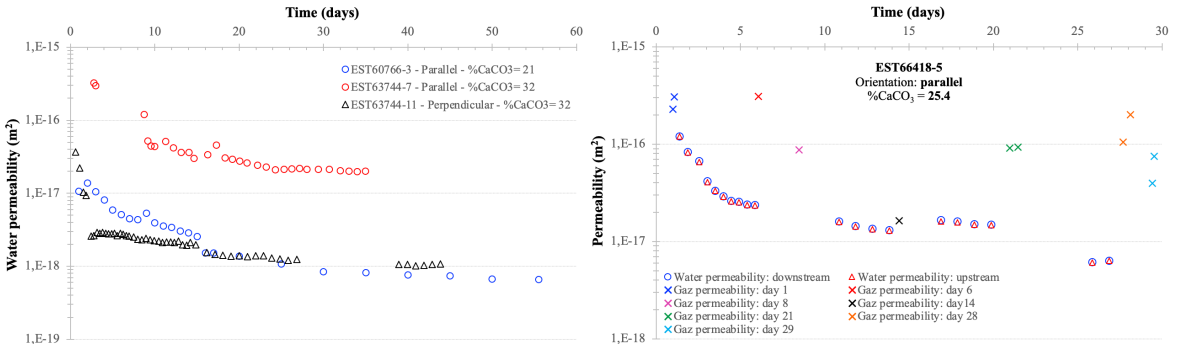

Figure 2. Evolution of crack water permeability during self-sealing tests on samples EST60766-3, EST63744-7 and EST63744-11 (left) and during self-sealing test on sample EST66418-5 (right).

3.2 Influence of sample orientation and calcite content on the self-sealing process

For Auvray et al. (2015) and Giot et al. (2019), there are three main processes implied in self-sealing. The first is swelling between smectite sheets (intra-particle or crystalline swelling) due to adsorption of water since the samples are a little desaturated initially. The second is inter-particle swelling due to osmotic effects by absorption of water between clay particles at higher water saturation (i.e., during self-sealing experiment). The last is plugging of the fractures by particle aggregation. Water penetrates more easily between the clay sheets in samples oriented in parallel to the bedding plane, thus initiating the self-sealing process more quickly. During these quick phases, there is a rapid decrease of the water permeability and the crack volume (Fig. 2, left). Then, there is a moderate and progressive decrease in water permeability and crack volume (Figs. 3) due to the progressive swelling of smectite clay minerals in the whole sample and the expansion and densification of clay plugs in the central crack. For parallel samples, clay minerals can swell freely laterally towards the inside of the fracture without any constraint whereas for perpendicular samples, the axial contraction (due to the 4MPa confining pressure) prevents probably a free swelling of the clay minerals surfaces in the axial direction. From these first results, it seems surprisingly that the self-sealing process is not more efficient for the parallel sample (i.e., when the bedding plane is parallel to the fracture surface). The (crystalline and osmotic) swelling mechanisms are certainly more efficient for the parallel samples, but the final phases of plugs formation, expansion and densification, which are maybe less dependent on the sample orientation, are possibly much more efficient to seal cracks.

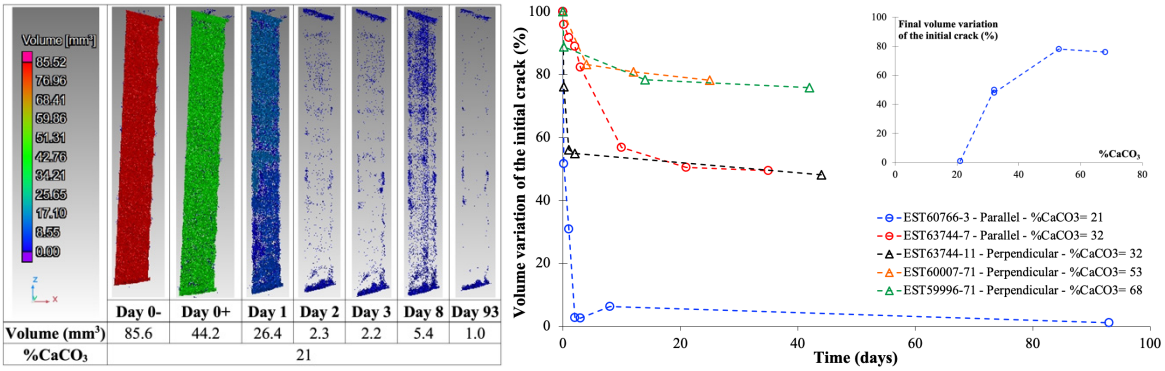

Figure 3. Left: X-ray 3D tomography images of parallel sample EST60766-3 showing the evolution of the crack volume with time during self-sealing test (Day 0-: after hydrostatic loading; Day 0+: after crack saturation). Right: Volume variation percentage of the initial crack (normalized with the volume after applying confining pressure) obtained from X-ray tomography 3D images during all self-sealing tests with water. Insert at the top right: volume variation percentage of the initial crack at the end of the test as a function of the calcite content.

The water permeability of clayey facies samples decreased significantly during self-sealing tests: from 10^{-17} to 7×10^{-19} m^2 in 55 days for sample EST60766-3, from 3×10^{-16} to 2×10^{-17} m^2 in 35 days for sample EST63744-7, from 4×10^{-17} to 1×10^{-18} m^2 in 44 days for sample EST63744-11. However, the initial permeability of the healthy (i.e., initial) claystone, which is almost 2 orders of magnitude lower (10^{-20} m^2 to 10^{-21} m^2) according to previous works (Escoffier 2002 and Homand et al. 2004), is never recovered. Moreover, the self-sealing process induces a significant reduction of the crack volume (Figs. 3). Concerning the samples with high calcium carbonate content (EST60007-71 and EST59996-71), self-sealing was very moderate and the fracture remained globally open (Fig. 3 right). Then, the calcite content, which is roughly anti-correlated with the clay content, has a strong impact on the physico-chemical sealing process in claystone. The higher the carbonate content, the slower the self-sealing process, whatever the sample orientation. The insert in Figure 4 represents the volume variation percentage of the initial crack at the end of the test as a function of the calcite content. It shows that the self-sealing capacity is strongly correlated to the calcite content. Our results support the work of Giot et al. (2019) where it is indicated that the threshold regarding the carbonate content to observe an effective self-sealing would be around 40%. This result highlights the importance of the mineralogy of the clay host rock to allow a good sealing of fractures in the EDZ during the resaturation of the underground structures for radioactive waste storage in clayey rocks.

3.3 Influence of gas injection on the self-sealing process

A self-sealing test was performed with nitrogen injections on sample EST66418-5 (parallel, %CaCO3 = 25.4) to determine the influence of an inert gas on the self-sealing process. The water and gas permeability of this specimen are presented in Fig. 2 (right). The scattering of gas permeability measurements may be explained by: the difficulty to obtain a measurable steady state gas flow (the time interval is not the same for all gas permeability measurements), the difficulty to apply and measure precisely low gas pressures (0.2 MPa or 0.5 MPa) at the bottom/upstream of the triaxial cell, the residual water inside the crack that can disturb the gas flow.

At the end of this self-sealing test, the water permeability is equal to 6×10^{-18} m^2, whereas the gas permeability is about 10^{-16} m^2. The water permeability decreases quite rapidly at the beginning like for the other tests (Fig. 2 left) but the decrease is slower thereafter. It seems that the injection of the gas slows down the decrease of the water permeability even though the crack is almost closed at the end of the experiment after 29 days (3.3 mm^3). This could be explained by the desaturation of the crack induced by the gas injection, which thus reduces the self-sealing process. The injection of an inert gas has therefore a retarding effect on the self-sealing process. This result has obviously to be confirmed by additional similar experiments.

4 CONCLUSIONS AND PERSPECTIVES

We used an X-ray transparent triaxial cell to perform self-sealing tests on artificially fractured core samples of Callovo-Oxfordian claystone. Two kinds of self-sealing tests were performed. First, self-sealing tests with water injection on samples with different orientations (parallel and perpendicular to the bedding plane) and calcite contents. Second, a self-sealing test with injection of both water and gas. 3D X-ray scans were performed before, during and after the experiments to assess the evolution of the crack volume. Fracture permeability (to water and gas) was measured continuously.

It resulted from our study that the higher the calcite content, the less effective the self-sealing process, whatever the sample orientation (parallel or perpendicular). An effective sealing requires a carbonate content lower than 40%. Moreover, it seems that the self-sealing process is equally efficient for both parallel and perpendicular orientations. Injection of an inert gas has a delay effect on the self-sealing process due to the crack desaturation. Generally, the self-sealing process is fast at the beginning of the test and then stabilizes after one month. The permeability of the COx claystone samples is partially restored compared to the initial permeability of the healthy claystone. It is all the more promising that the duration of our experiments is much shorter than the in-situ time scale.

These first results, which have to be confirmed with additional similar experiments, are very promising and give confidence to the positive impact of the self-sealing process on the restoration of the initial mechanical and hydraulic (i.e., sealing) properties of the COx claystone. This physico-chemical mechanism will allow a good sealing of fractures in the EDZ during the resaturation of the underground structures for radioactive waste storage, which will guarantee the safety of the site.

ACKNOWLEDGEMENTS

This project has received funding from the European Union's Horizon 2020 research and innovation program under grant agreement No 847593 and from ANDRA (French National Radioactive Waste Management Agency). The experiments presented in this study were carried out with the experimental devices available in the HGM experimental platform (Université de Lorraine-CNRS – http://georessources.univ-lorraine.fr/fr/content/hydrogeomecanique).

REFERENCES

Auvray, C., Grgic, D., Morlot, C., Fourreau, E., & Talandier, J. 2015. X-Ray Tomography Applied to Self-Healing Experiments on Argillites. In: *Proceedings of the 13th ISRM International Congress of Rock Mechanics*, Montréal, (Québec, Canada).

Bastiaens, W., Bernier, F., & Li, X. L. 2007. SELFRAC: Experiments and conclusions on fracturing, self-healing and self-sealing processes in clays. *Physics and Chemistry of the Earth*, Parts A/B/C, 32(8–14), pp. 600-615. DOI: 10.1016/j.pce.2006.04.026.

De La Vaissière, R., Armand, G., & Talandier, J. 2015. Gas and water flow in an excavation-induced fracture network around an underground drift: A case study for a radioactive waste repository in clay rock. *Journal of Hydrology*, 521, pp. 141–156. DOI: 10.1016/j.jhydrol.2014.11.067.

Escoffier, S. 2002. *Caractérisation expérimentale du comportement hydromécanique des argilites de Meuse/Haute-Marne*. Ph.D. thesis. Institut National Polytechnique de Lorraine, France.

Giot, R., Auvray, C., & Talandier, J. 2019. Self-sealing of claystone under X-ray nanotomography. *Geological Society, Special Publications*, 482(1), pp. 213–223. DOI: 10.1144/SP482.4

Homand, F., Giraud, A., Escoffier, S., Koriche, A., & Hoxha, D. 2004. Permeability determination of a deep argillite in saturated and partially saturated conditions. *International Journal of Heat and Mass Transfer*, 47(14), pp. 3517–3531. DOI: 10.1016/j.ijheatmasstransfer.2004.02.012.

Klinkenberg, L. J. 1941. The permeability of porous media to liquids and gases. In: *Drilling and production practice* , pp. 200–213.

Van Geet, M., Bastiaens, W., & Ortiz, L. 2008. Self-sealing capacity of argillaceous rocks: Review of laboratory results obtained from the SELFRAC project. *Physics and Chemistry of the Earth*, Parts A/B/C, 33, pp. S396–S406. DOI: 10.1016/j.pce.2008.10.063.